We are IntechOpen,
the world's leading publisher of
Open Access books
Built by scientists, for scientists

4,800
Open access books available

122,000
International authors and editors

135M
Downloads

Our authors are among the

154
Countries delivered to

TOP 1%
most cited scientists

12.2%
Contributors from top 500 universities

CLARIVATE ANALYTICS
BOOK CITATION INDEX
INDEXED

WEB OF SCIENCE™

Selection of our books indexed in the Book Citation Index
in Web of Science™ Core Collection (BKCI)

Interested in publishing with us?
Contact book.department@intechopen.com

Numbers displayed above are based on latest data collected.
For more information visit www.intechopen.com

Thermal Oxidation of Silicon Carbide (SiC) – Experimentally Observed Facts

Sanjeev Kumar Gupta and Jamil Akhtar
*Central Electronics Engineering Research Institute (CEERI)/ Council of Scientific and
Industrial Research (CSIR)
India*

1. Introduction

The thin thermally grown SiO_2 plays a unique role in device fabrication of Si-VLSI Technology. The well established growth mechanisms and continuous research to grow high quality SiO_2 on Si substrate has to lead the development of planner-Technology and permits the fabrication of well defined diffused or ion-implanted junctions of precisely controllable dimensions. Among the all wide bandgap semiconductors, Silicon Carbide (SiC) is the only compound semiconductor which can be thermally oxidized in the form of SiO_2, similar to the silicon growth mechanism. This means that the devices which can be easily fabricated on Si substrate (Power MOSFET, IGBT, MOS controlled thyristor etc.) can also be fabricated on SiC substrate. Moreover, a good knowledge of SiO_2/Si interface has been established and has to lead great progress in Silicon-Technology that can be directly applied to development of SiC-Technology.

Similar to the Silicon-Technology, high quality thin SiO_2 is most demanded gate oxide from the SiC based semiconductor industries to reduce the cost and process steps in device fabrication. Various oxidation processes has been adopted such as dry oxidation [1], wet oxidation [2], chemical vapour deposition (CVD) [3], and pyrogenic oxidation [4-6] in order to achieve the most suitable process to realize the SiC-based MOS structures. To develop the basic growth mechanism of SiO_2 on SiC surfaces apart from the Si growth mechanisms, worldwide numbers of researchers are intensively working on the above specified problems. Since SiC is a compound material of Si and C atoms, that is why the role of C atoms during the thermal growth of SiO_2 has been observed to be very crucial. Several studies [7-9] confirm the presence of C species in the thermally grown oxide, which directly affect the interface as well as dielectric properties of metal-oxide-semiconductor structures [10]. For this reason, rigorous studies on electrical behavior of thermally grown SiO_2 on SiC play a fundamental role in the understanding and control of electrical characteristics of SiC-based devices. It has been reported that the growth rate of SiC polytypes is much lower than that of Si [11-13]. The rate of reaction on the surface of SiC is much slower than that of Si under the same oxidation conditions. In case of SiC, another unique phenomenon has been observed that the oxidation of SiC is a face terminated oxidation, means the both polar faces (Si and C face) have different oxidation rates [14-15]. These oxidation rates are also depend on the crystal orientation of SiC and polytypes i.e. Silicon carbide shows an anisotropic oxidation nature.

2. Specification of used 4H-SiC substrate

The availability of the right kind of material has put a restriction for the fabrication of semiconductor devices. There are limited sources where single crystalline SiC substrate is available. At present, the most known firm is M/s CREE Research Inc USA, which is known worldwide for the supply of basic SiC substrates in 2″ or larger diameter sizes. In this reported work n-type 4H-SiC material was the obvious selection with maximum possible epitaxy layer (50 µm) on Si-face with lowest possible doping. Accordingly, CREE Research Inc. USA supplied the following structure on a 2″ diameter wafer. Figure 1 (a) shows the schematic details of used 4H-SiC substrate and (b) shows the 2″ wafer hold by tweezers showing optical transparency by looking at carrier holder through the wafer.

3. Kinetics of thermal oxidation

3.1 Thermal oxidation setup

Thermal oxidation is the proficient process in VLSI technology which is generally carried out in oxidation furnace (or diffusion furnace, since oxidation is basically based on the diffusion mechanism of oxidizing agent) that provides the sufficient heat needed to elevate the oxidizing ambient temperature. The furnace which was used for thermal growth of SiO_2 on 4H-SiC is typically consisted of:

1. a fool proof cabinet
2. a heating assembly
3. a fused quartz horizontal process tubes where the wafers undergo oxidation
4. a digital temperature controller and measurement system
5. a system of gas flow meter for monitoring involved gases into and out of the process tubes and
6. a loading station used for loading (or unloading) wafers into (or from) the process tubes as shown in figure 2.

The heating assembly usually consists of several heating coils that control the temperature around the furnace quartz tube. There are three different zones in the quartz tube i.e. left, right and center. The temperature of both end zones (left and right) was fixed at $400^0C \pm 50^0C$ throughout the process. For the ramp up and ramp down of furnace temperature, there are three digital control systems for all three zones. The furnace consists of two different gas pipe lines, one is for N_2 gas and other is for dry/wet O_2 gas. To control the gas flow, there are MATHESON'S gas flow controllers. A quartz bubbler has been used to generate the steam using highly pure DI-water. There is a temperature controller called heating mental to control the temperature of bubbler. Wet oxygen as well as dry oxygen or dry nitrogen has been passed through a quartz nozzle to the quartz furnace tube.

3.2 Sample preparation

The cleaning procedure, which is generally used in Si-Technology, has been adopted for this work. All chemicals used in wet-chemical procedure were MOS grade. The wafers were treated for all three major chemical cleaning procedures i.e. Degreasing, RCA and Piranha. Degreasing has three conjugative cleaning steps. First, the wafers were dipped in 1, 1, 1-Trichloroethane (TCE) and boiled for ten minutes to remove the grease on the surface of wafers. Second, the wafers were dipped in acetone and boiled for ten minutes, to remove
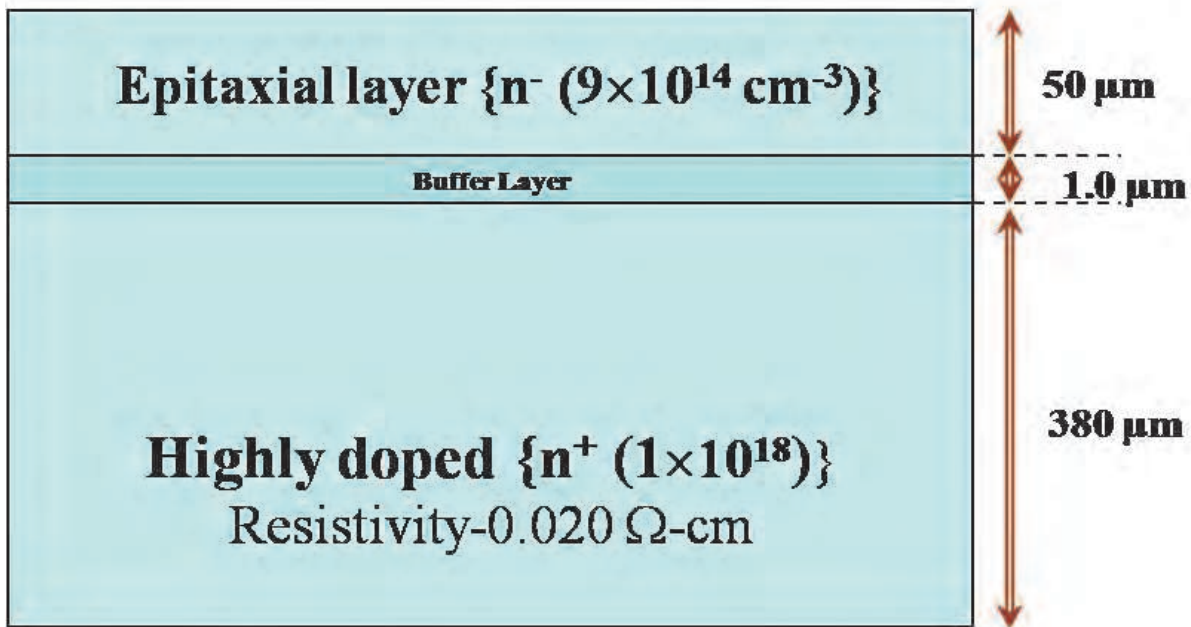
(a)
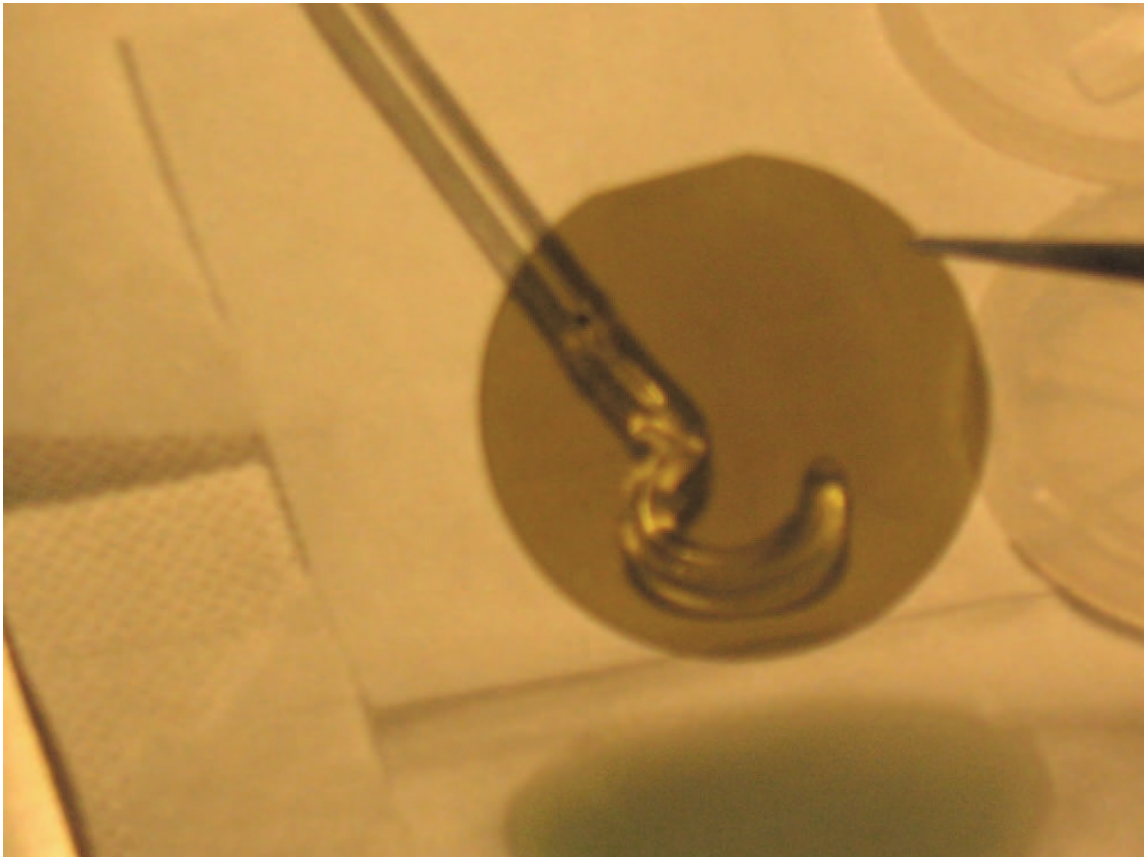
(b)

Fig. 1. (a) Schematic details of 4H-SiC substrate which was used and (b) A 2″ diameter 4H-SiC wafer hold by tweezers showing optical transparency by looking at carrier holder through the wafer
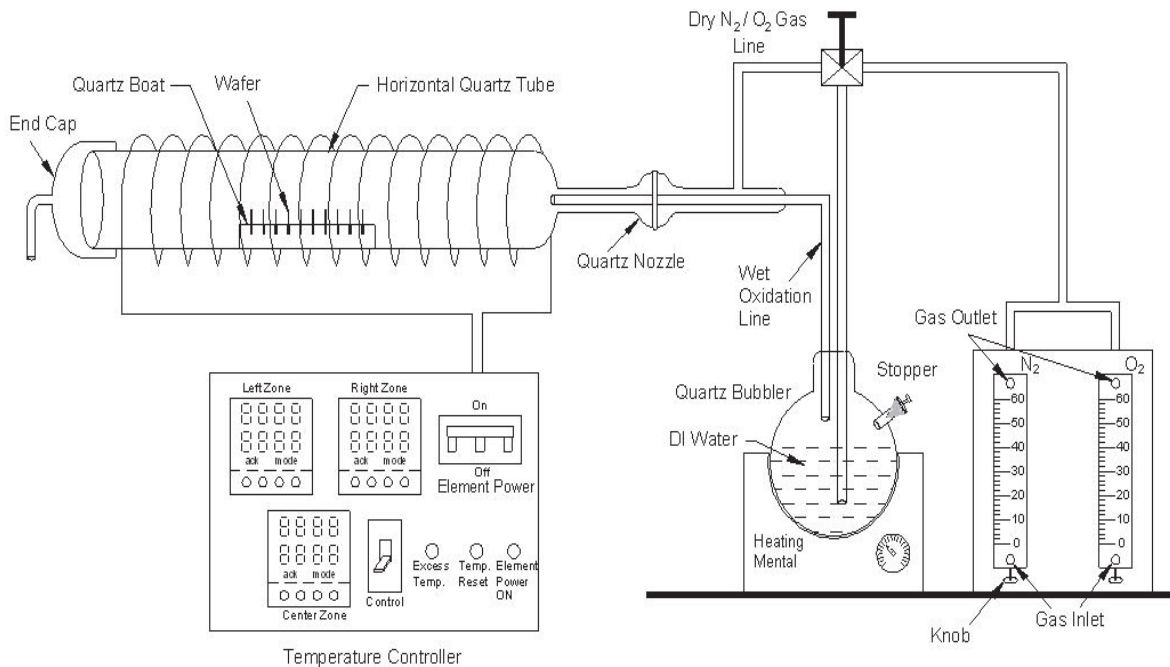
Fig. 2. Schematic diagram of horizontal oxidation furnace

light metal ions. Third, the wafers were dipped in methanol and boiled for ten minutes. Then the wafers were rinsed in de-ionized (DI) water. Subsequently, the standard Radio Corporation of America (RCA) cleaning procedure was followed. This process consisted of two stages, which is termed as standard cleaning-1 (SC-1) and SC-2. In SC-1, the wafers were dipped in high pH alkaline mixture (NH_4OH, H_2O_2 and DI-water) in the ratio of (1:1:5) at some temperature for 10 minutes. There are three main purpose of SC-1: (1) to remove the organic substances on the 4H-SiC wafer surface due to wet oxidation effect, (2) to expose the surface so that any trace metals can be desorbed, and (3) to enable hydrous oxide film to form and dissolve continuously. After SC-1, the wafers were thoroughly ringed in DI-water and then dipped in 10% hydrofluoric (HF) acid for one minute to etch off any remaining SiO_2 (native oxide). The SC-2 consisted of a mixture of (HCl, H_2O_2 and DI-water) in the ratio of (1:1:6). The wafers were dipped in the mixture for 10 minutes at some temperature followed by thoroughly ringed in DI-water and native oxide removal using 10% HF solution. The SC-2 cleaning process could able to dissolve alkali ions, water insoluble hydro oxide compounds and any dual trace metals that was unable to disrobe by SC-1. The last cleaning treatment is known as Piranha cleaning. The piranha solution consisted of a mixture of (H_2SO_4 and H_2O_2) in the ratio of (7:1). Then wafers are dipped in this solution for 15 minutes to remove any heavy metal resident on the wafer surface. Finally, the wafers were thoroughly rinsed in DI- water which, is followed by 10% HF dip.

3.3 Oxidation methodology

Thermal oxidation process was divided into six groups of different temperature range starting from 1050⁰C to 1150⁰C for different oxidation time i.e. 30, 60, 90, 120, 150 and180 minutes. The both oxidizing ambient (steam and dry) had been tried to analyze the exact behavior of thermal oxidation on both faces of 4H-SiC. The wafers were placed in quartz glassware known as boats, which are supported by fused silica paddles inside the process tube of the center zone. A boat can contain many wafers. The oxidizing agent comes with the contact of wafers

and diffusion take place at the surface of substrate. This diffusion mechanism is resulted into a vast variation in oxidation rate. In the experiment of wet oxidation the temperature of quartz bubbler (filled with DI water) is always kept at constant 85^0C. 0.4 LPM (liter per minutes) flow of wet molecular oxygen has been maintained in the helical path through out the process tube. While in the experiment of dry oxidation, a continuous flow of constant dry oxygen is maintained throughout the process. The samples of each group were loaded and unloaded at 800^0C in the 1.9 LPM flow of nitrogen for different time as described above, the ramp up and ramp down temperature of furnace $5^0C/min$ as shown in figure 3.

Wet/dry Oxidation at 1000^0C, 1050^0C, 1110^0C, 1150^0C

Time 0.5 H to 6H with step 0.5H

Load
{800^0C}

Unload
{800^0C}

Room Temperature
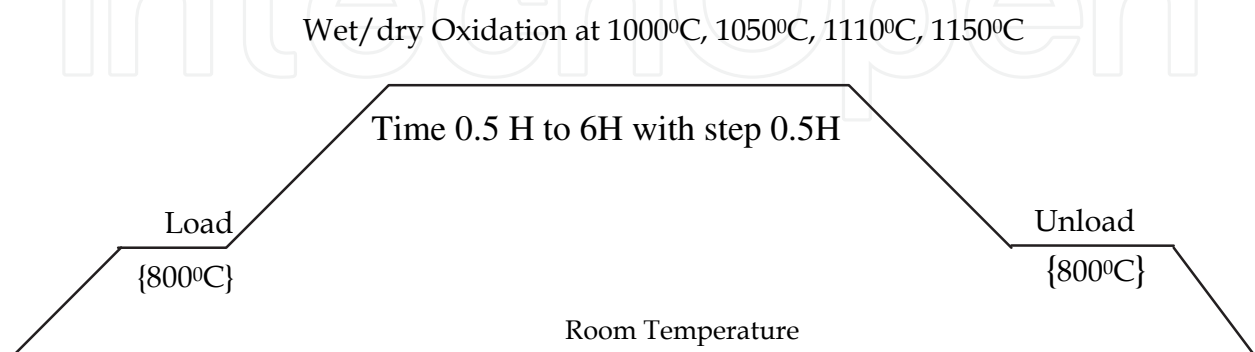
Fig. 3. Process flow of wet thermal oxidation

3.4 Determination of oxide thickness

The thickness of thermally grown oxide on both terminating faces was experimentally captured by ellipsometry technique followed by DAKTEK surface profiler verification.

3.4.1 Basic principle of ellipsometry

In ellipsometry technique a polarized coherent beam of light is reflected off the oxide surface at some angle. In this experiment, He-Ne Laser (6328 Å), was used as a source. The monochromatic light passes through a polarizing prism, which results in linearly polarized light. The polarization of light is changed by the reflection so it is now elliptically polarized. The reflected polarized light is then passed through another prism which is rotating about the axis of the light and finally onto a photodetector. This light is now reflected off of the sample which we wish to study. The reflected light intensity is measured as a function of polarization angle. By comparing the incident and reflected intensity and the change in the polarization angle, the film thickness was estimated. The output of the photodetector is displayed on a computer monitor. The principle of operation of an ellipsometer is illustrated by the schematic drawing of the ellipsometer shown in the figure 4 below.

3.4.2 Basic principle of surface profiler

The profiler has sharply, pointed, conical diamond with a rounded tip stylus, resting lightly on the surface, is traversed slowly across it, and the up and down movement of the stylus relative to a suitable datum are magnified and recorded on a base representing the distance traversed, a graph representing the cross-section will be obtained. Figure 5 shows the schematic diagram of surface profiler. Figure 6 (a) shows a sharp step on the oxidized surface which has been realized by photolithography. Figure 6 (b) shows the experimentally measured thickness of test sample.
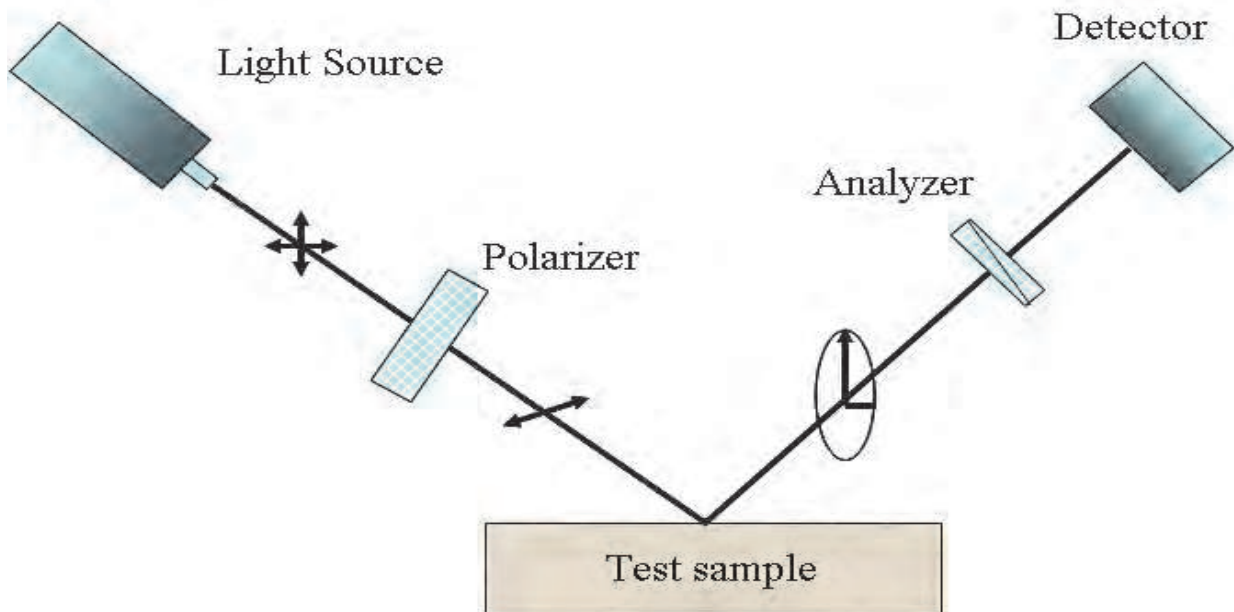
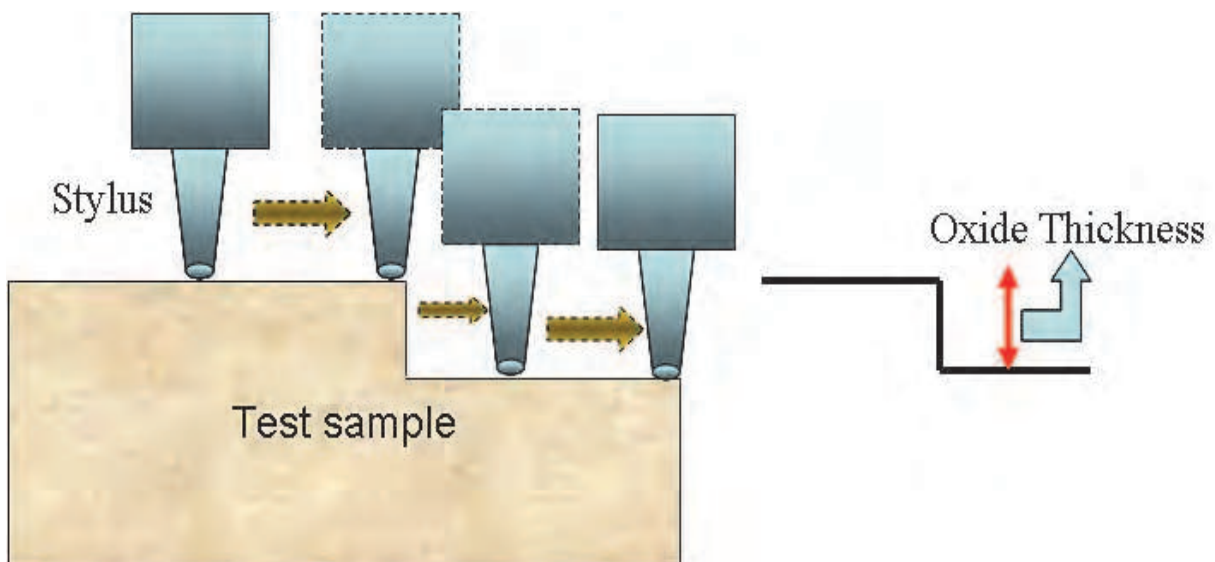Fig. 4. Schematic drawing of an ellipsometer

Fig. 5. Schematic drawing of surface profiler
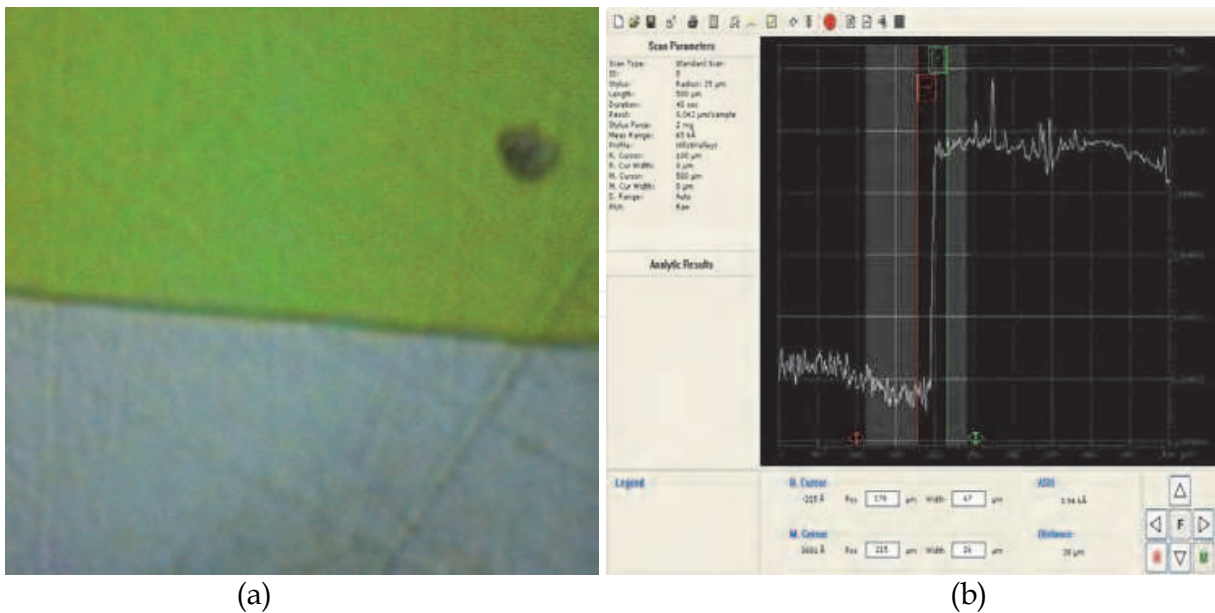
(a) (b)

Fig. 6. (a) Oxide step on 4H-SiC (b) Oxide thickness measurements using surface profiler

The measured oxide thickness was plotted as a function of oxidation time, which is shown in figure 7 and 8. The measured thickness was verified by surface profiler also.

4. Basic growth mechanism of 4H-SiC

The thermal oxidation growth mechanism of SiC is described by same rules as Si, which is well explained by Deal and Grove [16] with some modifications. Finally, the growth rate equation (linear-parabolic) is the same as explained for Si-oxidation. During thermal oxidation of silicon carbide most of the excess carbon is believed to be removed from the interface through the formation of CO_2, which diffuses through the oxide and is thereafter released from the sample surface. However, some of the carbon can remain within the oxide and form carbon clusters or graphitic regions. Such regions near the SiO_2/SiC are expected to be electrically active and could be responsible for the interface states [17]. The process of SiC thermal oxidation can be divided into three steps. First, the oxidation of the SiC surface occurs through the interaction of an oxygen atom into the chemical bond of a SiC molecule. This oxygen insertion creates a Si-O-C species, which then splits into a CO molecule and a Si atom with a dangling bond. These CO molecules diffuse through the oxide of the oxide surface and react with an oxygen atom, creating CO_2. Second, the Si atom reacts with oxygen atoms, which are at the SiC surface in the initial oxidation or diffuses through the oxide to the oxide SiC interface, forming SiO_2. These three processes can be summarized by the following reactions:

$$SiC + O \rightarrow CO + Si$$
$$CO + O \rightarrow CO_2$$
$$Si + 2O \rightarrow SiO_2$$
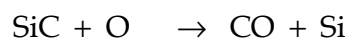
Contrary to the relatively simple oxidation of Si, there are five major steps in the thermal oxidation of SiC.
1. transport of molecular oxygen gas to the oxide surface
2. in-diffusion of oxygen through the oxide film
3. reactions with SiC at the oxide/SiC interface

4.   Out-diffusion of product gases (e.g., CO_2) through the oxide film and
5.   removals of product gases away from the oxide surface.

The last two steps are not involved in the oxidation of Si. The oxidation of SiC is about one order of magnitude slower than that of Si under the same conditions. The first and last steps are rapid and are not rate-controlling steps. But among the remaining steps, the rate-controlling step is still uncertain as discussed in several articles [12]. It has been reported in various research papers that the thermal growth kinetics of SiC is governed by linear parabolic law of Deal and Grove, as derived for Silicon [12] [18-20].

$$X_0^2 + AX_0 = B(t+\tau) \tag{1}$$

Where, X denotes the oxide thickness and t is oxidation time. The quantity τ corresponds to a shift in the time coordinate that correct for the presence of the initial layer of oxide thickness and A and B are constants. The above equation is a quadratic equation. The solution of equation can be written as

$$\frac{X_0}{A/2} = \left(1 + \frac{t+\tau}{A^2/4B}\right)^{1/2} - 1 \tag{2}$$

In order to observe the experiment more precise, four numbers of samples were oxidized at same temperature for same oxidation time. All obtained values of thickness are statistically plotted as the function of oxidation time, which is shown in figure 7 (Si-face) and Figure 8 (C-face).
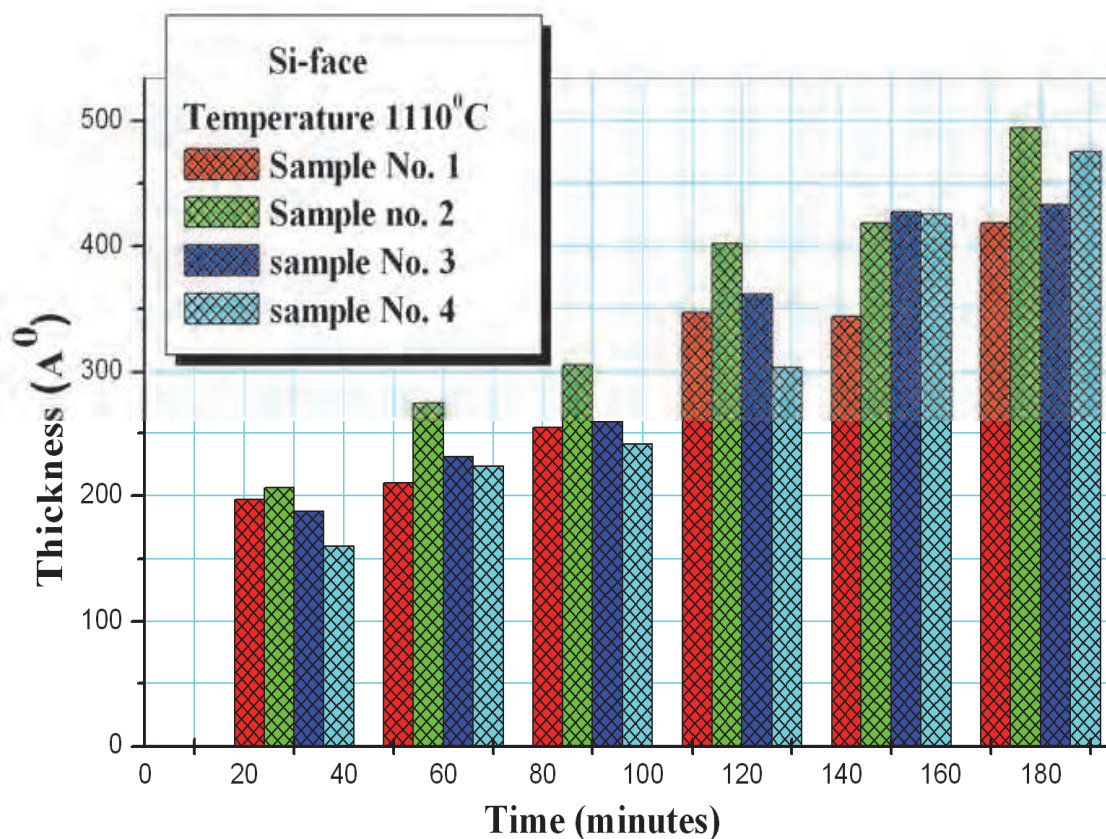

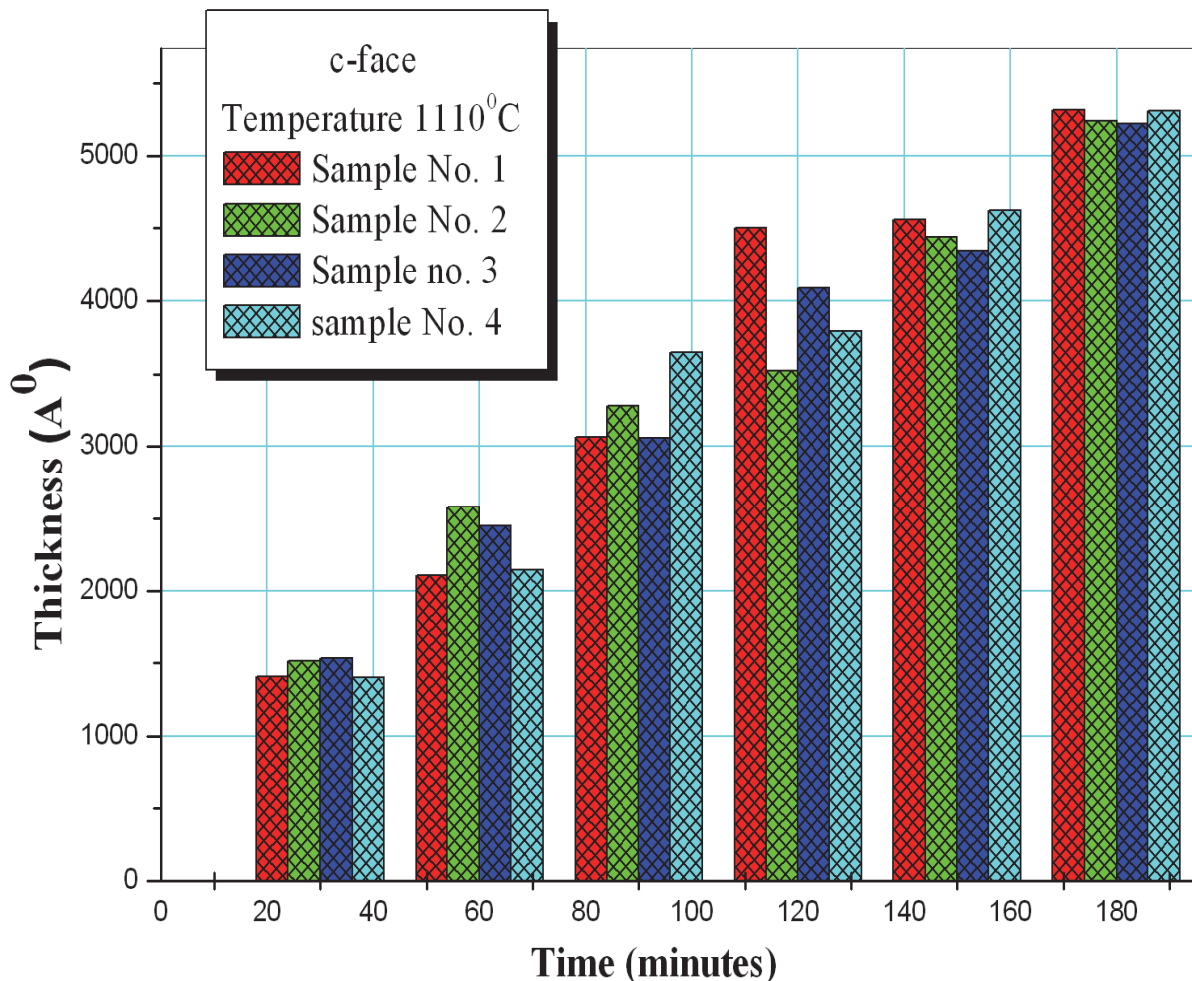Fig. 7. Growth of thermal oxide on Si-face

Fig. 8. Growth of thermal oxide on C-face

There are two limiting case of equation 2
1. For long oxidation time i.e. thick oxidation Equation 2 becomes

$$X_0{}^2 = Bt \qquad (3)$$

This relation is called parabolic law and B is called parabolic rate constant. This limiting case is diffusion controlled case because diffusion flux becomes small in comparison to the substrate surface reaction flux. Here the rate of oxidation is limited by the availability of oxidant at the Si rich interface as well as C rich interface, which is controlled by the diffusion process.
2. For short oxidation time i.e. thin oxide equation 2 can be written as

$$X_0 = \frac{B}{A}(t + \tau) \qquad (4)$$

This relation is called linear law and the quantity B/A is called the linear rate constant because in this case enough oxidant is transported across the oxide layer, and the oxidation rate is controlled by concentration of oxidant at the surface [21].
Wet thermal oxidation of the C-face of 4H-SiC is systematically slower than that of Si for identical conditions of temperature, pressure and time. Since the oxidation rate has been

shown to depend only feebly on the polytypes for the Si-face and not at all for the C-face. It is realistic to believe that although there may be small quantitative differences between the oxidation processes of different polytypes along the perpendicular directions to the bilayer stacking units. The main processes involved in oxidation are diffusion, interface reaction rates and so on, should be largely analogous, and so it is practical to discuss oxidations mechanisms without paying special attention to the polytypes. Figure 9 shows the quantitative oxide thickness up to 6 hours after analyzing the growth dynamic as explained above at 1110⁰C. A number of oxidation experiments have been repeated in order to verify the previously obtained results. Wet and dry thermal oxidations have been performed separately at the different temperature. Figure 10 (a, b, c and d) shows the experimentally measured thermal oxide thickness at the different temperature as explained above by the method of wet and dry oxidation on Si as well as C-face. In both cases (dry and wet), a face terminated behavior has been observed means C-face always oxidized faster than that of Si-face under same oxidation condition. This discrepancy in growth rate is termed as growth rate multiplication factor (GRMF), means how much oxidation on C-face is faster than that of Si-face. A very simple equation has been formulated by just dividing the oxide thickness on C-face to oxide thickness on Si-face (equation 5).

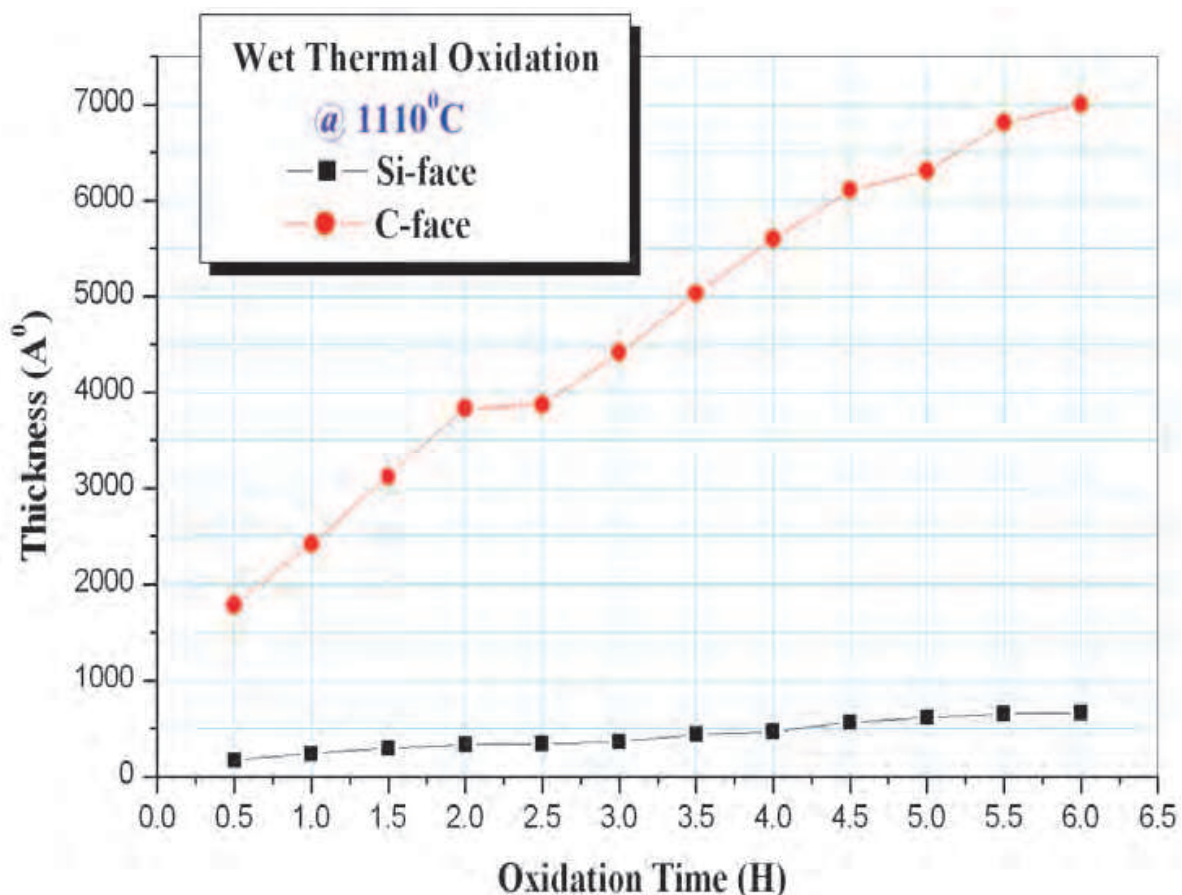$$GRMF = \frac{X_0\big|_{C-face}}{X_0\big|_{Si-face}} \tag{5}$$

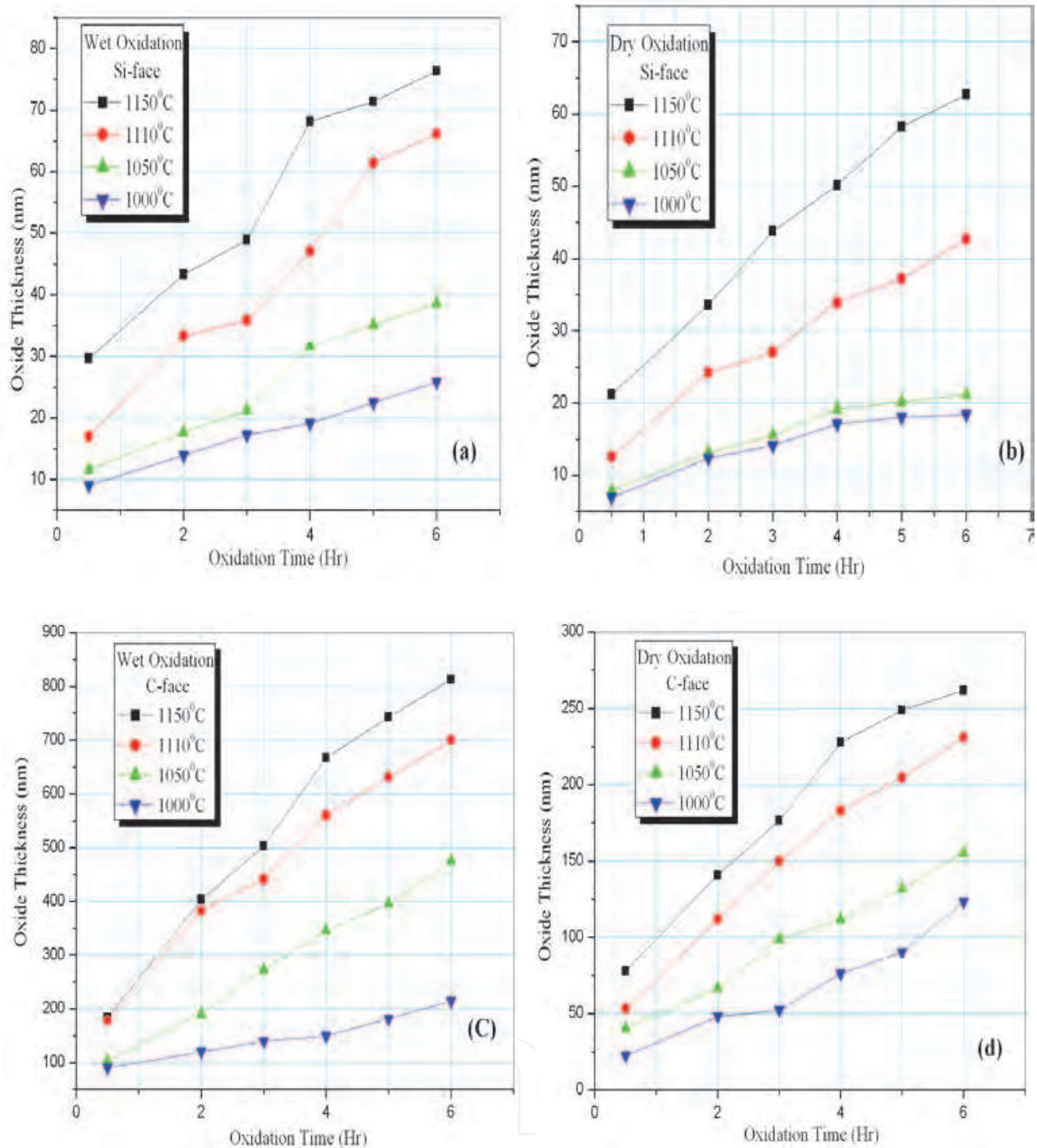Fig. 9. Experimental growth of wet thermal oxide on both terminating face

Fig. 10. (a) Plots of oxide growth profile on Si-face by wet oxidation, (b) by dry oxidation, (c) wet oxidation on C-face and (d) dry oxidation on C-face

The growth rate multiplication factor (GRMF) on both terminating faces has been calculated as a function of oxidizing ambient (dry and wet). It was observed that in case of dry oxidation GRMF is found in the range of 4-6, means in case of dry oxidation C-face oxidize 4 to 6 times faster than that of Si-face. In the similar way for wet oxidation this GRMF is found in the range of 8-12, means in case of wet oxidation C-face oxidize 8 to 12 times faster than that of Si-face. Figure 11 shows the experimentally measured GRMF in both oxidizing ambient.
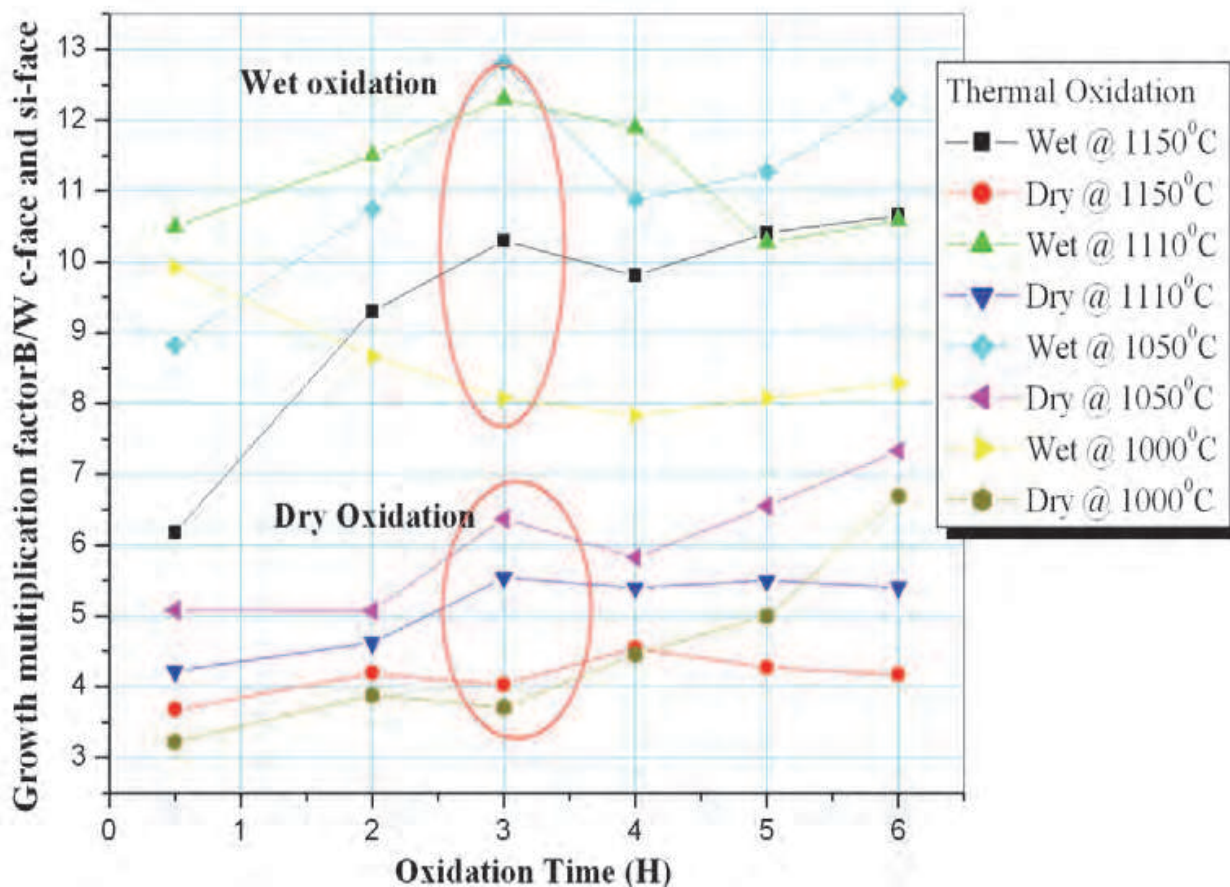
Fig. 11. Determination of growth rate multiplication factor between both terminating faces by the method of wet and dry oxidation process

5. Determination of average growth rates

We have applied the Deal and Grove oxidation model to the relations between oxide thickness X and oxidation time t. The quantitative values of the linear parameters B/A and parabolic parameter B in the Deal–Grove equation has been used by fitting to the calculated curve to the observed values in the entire thickness range. The fits are in general good at all of the oxidation temperatures. However, to observe the growth rate behavior for both terminating faces, the grown oxide is divided by its oxidation time. We have derived the oxidation rates dX_0/dt as a function of oxide thickness for dry as well as wet oxidation on both terminating faces. Since we are calculating the growth rate of all samples after each successive experiment that's why we are calling it average growth rate.

$$\left.\frac{dX_0}{dt}\right|_{sample1} \Rightarrow Average \left.\frac{dX_0}{dt}\right|_{sample1} \tag{6}$$

Figure 12 (a, b, c and d) shows the values of dX_0/dt as a function of oxide thickness (grown by the method of wet oxidation) at various oxidation temperatures. We have successfully obtained the values of the oxidation rate even in the thin oxide thickness range of less than 10 nm by these experiments. Figure 13 (a, b, c and d) shows the values of dX_0/dt as a function of oxide thickness (grown by the method of wet oxidation) at various oxidation
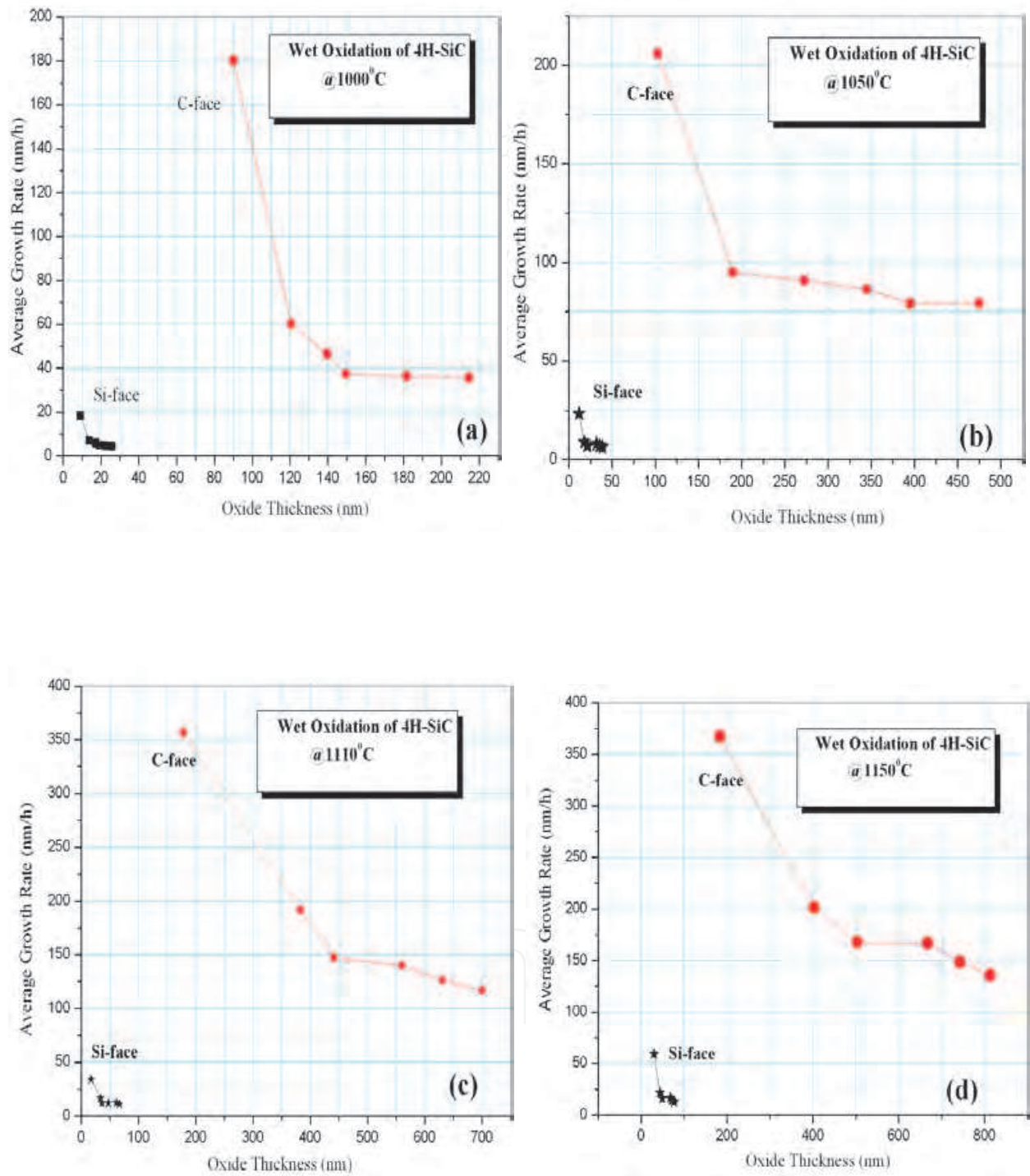
Fig. 12. (a) Plots of face terminated wet oxidation growth rate at 1000⁰C, (b) at 1050⁰C, (c) at 1110⁰C and (d) at 1150⁰C
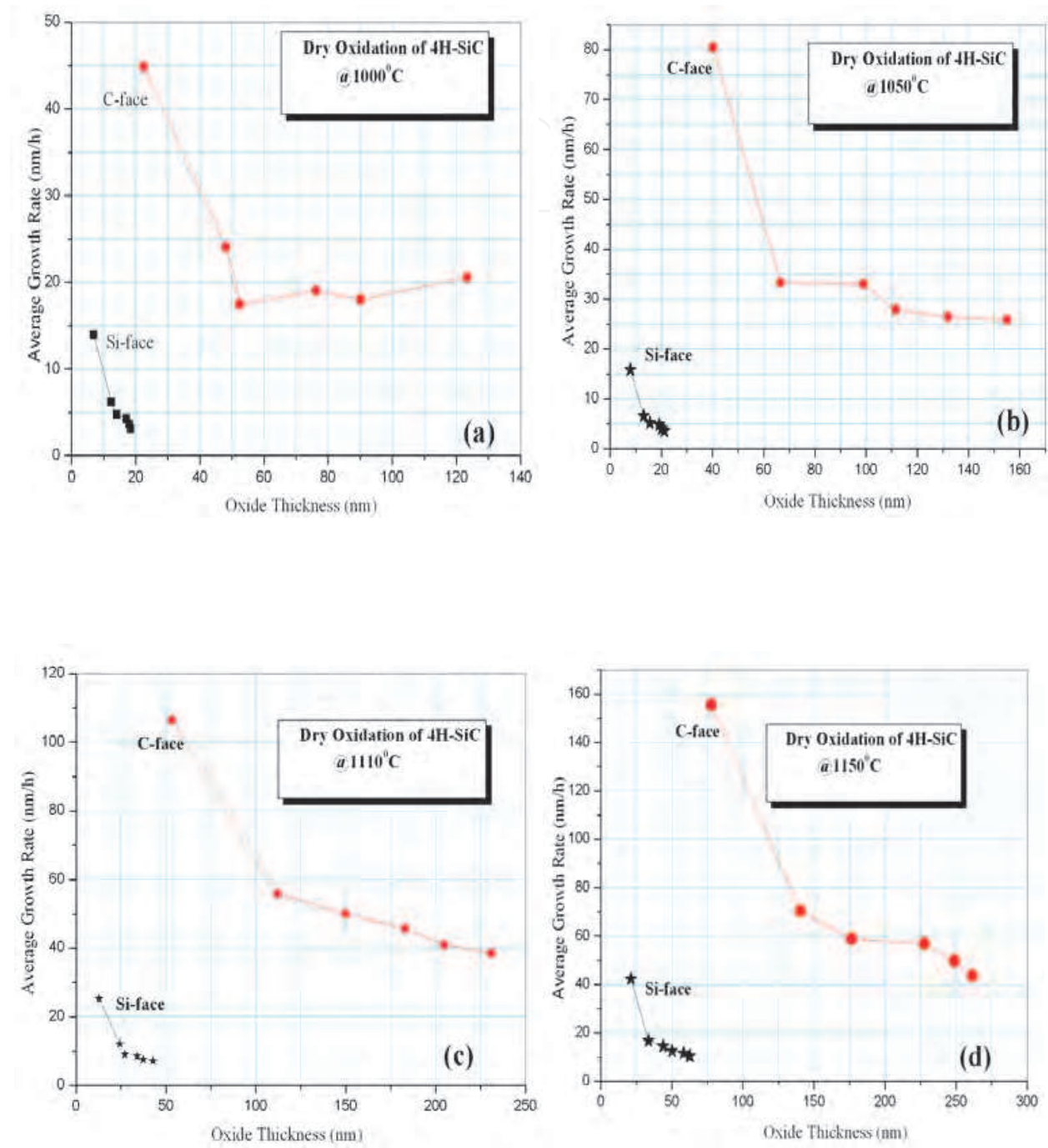
Fig. 13. (a) Plots of face terminated dry oxidation growth rate at 1000°C, (b) at 1050°C, (c) at 1110°C and (d) at 1150°C

temperatures. Initial oxide growth rate of 19, 24, 35, 67 nm/h (on Si-face) while 180, 220, 357, 374 nm/h (on C-face) have been calculated at 1000⁰C, 1050⁰C, 1110⁰C and 1150⁰C respectively. Similarly, thermal oxide growth for dry oxidation has been found to be 12, 17, 25, 42 nm/h (on Si-face) while 44.5, 81, 113, 157 nm/h (on C-face) have been calculated at 1000⁰C, 1050⁰C, 1110⁰C and 1150⁰C respectively. However, in the smaller thickness range, the values of dX_0/dt are not constant but increases with decreasing oxide thickness, i.e., the oxide growth rate enhancement occur at any temperature in this study in both case (Si-face and C-face). It is evident from the above data that the nature of growth rate is parabolic for all cases and initial average growth rate for wet oxidation is faster than that for dry oxidation. C-face is having the higher growth rate than that of Si-face at each oxidation temperature in both oxidations ambient. Figure 14 show the face terminated growth rate, revealing that the average growth rates of dry and wet oxide on Si-face is slower than that of C-face.
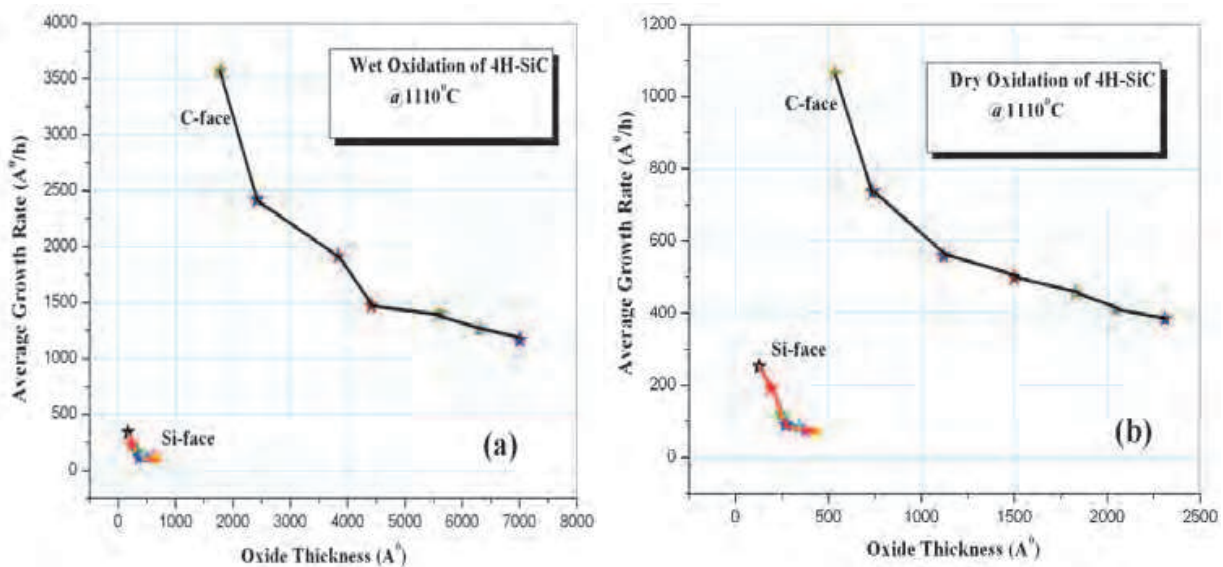

Fig. 14. Plots of oxidizing ambient terminated growth rate in wet oxidation and (b) in dry oxidation

6. Determination of rate constants

Thermal oxide growth rate constants have been determined by fitting the experimentally measured curve to the measurement made by Deal and Grove (as explained above) of oxide thickness as a function of oxidation time at various oxidation temperatures. In this experiment dry and wet thermal oxidation has been performed (as explained in section 2.3) at1000⁰C, 1050⁰C, 1110⁰C and 1150⁰C for different oxidation time. In each individual experiment, the value of τ has been fixed to zero for all temperature range. A plot of oxide thickness (X_0) versus t/X_0 from equation 1 should yield a straight line with intercept –A and slope B. Figure 15 (a) and Figure 15 (b) shows the X_0 versus t/X_0 plots of wet oxidation on Si-face (figure a) and C-face (figure b) of 4H-SiC. It has been observed that the absolute value of A increasing with decreasing oxidation temperature. At the same condition, the slope of the plots increases with increasing temperature. Measured values of these constants from the figure 15 are listed in table 1.
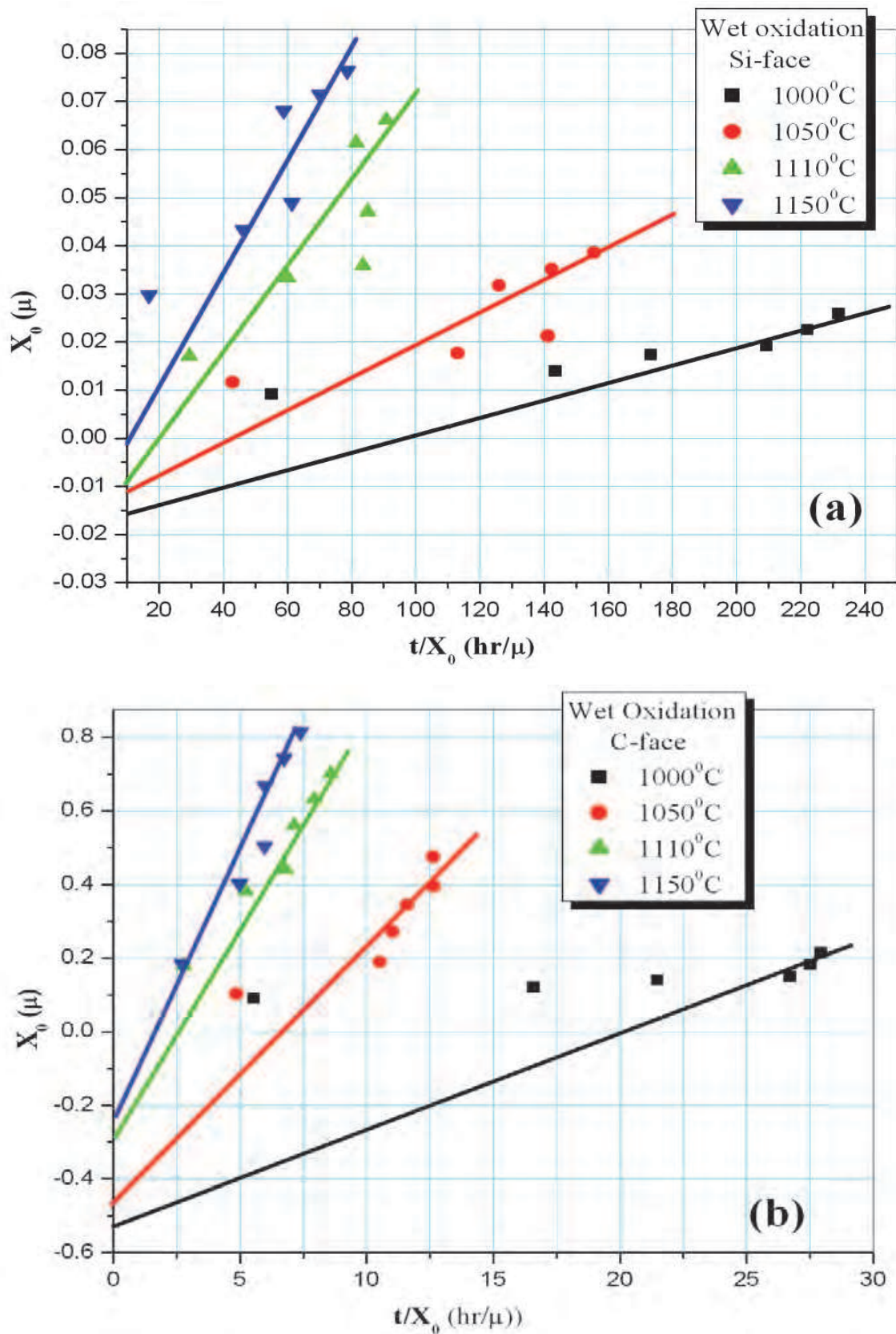
Fig. 15. (a) Experimentally measured curve of X_0 versus t/X_0 for wet oxidation on Si-face and (b) on C-face

Figure 16 (a) and 2.16 (b) are the again X_0 and t/X_0 for face terminated (Si-face and C-Face) oxidation in dry ambient at different oxidation time. The plots are straight line again (as shown in figure 16) with intercept –A and slope B. The measured linear as well as parabolic rates constant are listed in table 2.
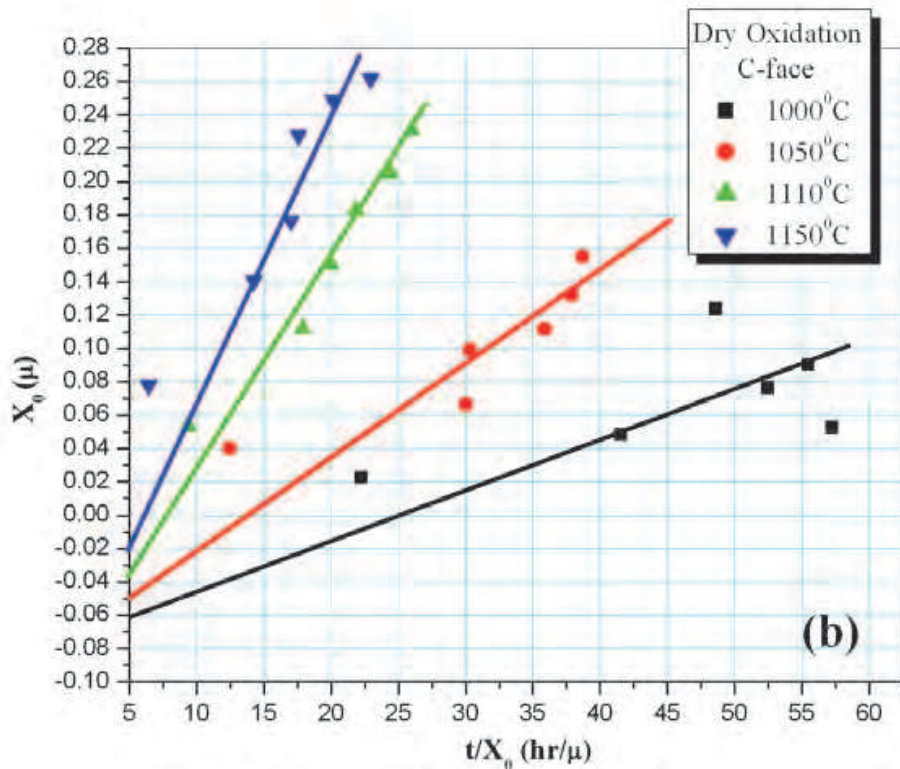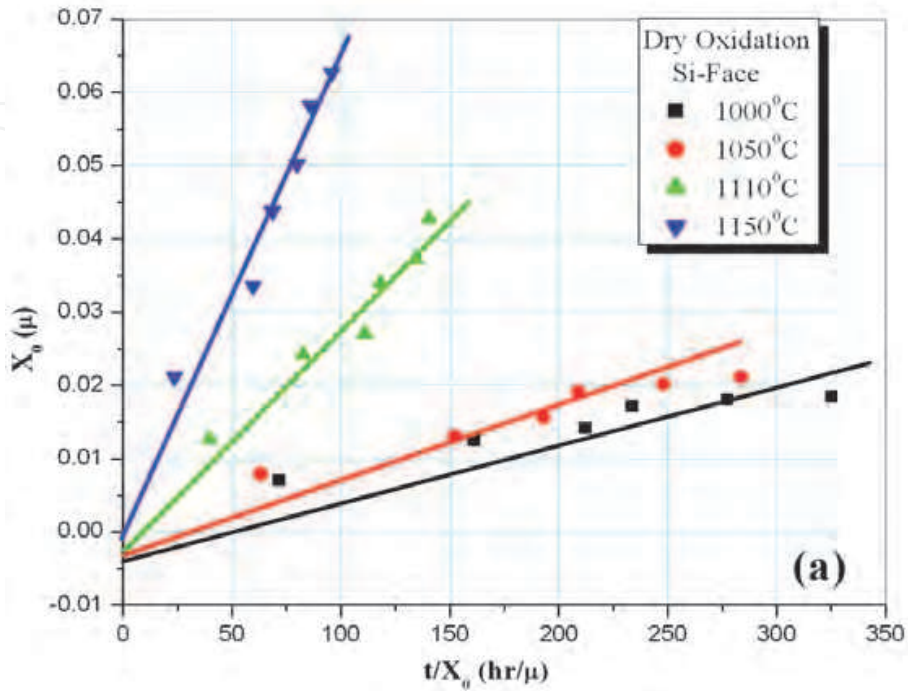

Fig. 16. (a) Experimentally measured curve of X_0 versus t/X_0 for dry oxidation on Si-face and (b) on C-face

Temperature (⁰C)	1000	1050	1110	1050
Si-face (Dry oxidation)	0.0000748	0.0001035	0.0003021	0.0006130
C-face (Dry oxidation)	0.00309	0.00568	0.01251	0.01711
Si-face (Wet oxidation)	0.000158	0.00033088	0.0008830	0.00120
C-face (Wet oxidation)	0.02571	0.06825	0.11303	0.14207

Table 1. Experimentally measured Parabolic Rate Constant (B)

Temperature (⁰C)	1000	1050	1110	1050
Si-face (Dry oxidation)	0.01533	0.02728	0.14081	0.58161
C-face (Dry oxidation)	0.05072	0.11643	0.34992	0.93078
Si-face (Wet oxidation)	0.01022	0.02916	0.10441	0.88499
C-face (Wet oxidation)	0.04887	0.14882	0.40398	0.61975

Table 2. Experimentally measured Linear Rate Constant (B/A)

7. Determination of activation energy

The rate of any reaction depends on the temperature at which it is run. As the temperature increases, the molecules move faster, and therefore, they collide more frequently to each other. As a result of these collisions, the molecules also carried more kinetic energy. Thus, the proportion of collisions that can overcome the activation energy for the reaction increases with temperature. The only way to explain the relationship between temperature and the rate of a reaction is to assume that the rate constant depends on the temperature at which the reaction is run. In 1889, Swedish scientist Svante Arrhenius showed that the relationship between temperature and the rate constant of a reaction. Arrhenius's research was a follow up of the theories of reaction rate by Serbian physicist Nebojsa Lekovic. Activation energy may also be defined as the minimum energy required to start a chemical reaction. The activation energy of a reaction is usually denoted by E_a, and given in units of kilojoules per mole or in eV.

$$K = Ze^{-\frac{E_a}{RT}} \tag{7}$$

Where, K is the rate constant for the reaction, Z is a proportionality constant that varies from one reaction to another, E_a is the activation energy for the reaction, R is the ideal gas constant in joules per mole kelvin, and T is the temperature in kelvin.

The Arrhenius equation can be used to determine the activation energy for a reaction. Taking the natural logarithm of both sides of the equation we get

$$\ln(K) = \ln(Z) - \frac{E_a}{RT} \tag{8}$$

This equation is then to fit as the equation for a straight line.

$$Y = mX + C \tag{9}$$

$$\ln(K) = -\frac{Ea}{R}\left(\frac{1}{T}\right) + \ln(Z) \tag{10}$$

According to this equation, a plot of ln (K) versus 1/T should give a straight line with a slope of - E_a/R, from which the value of activation energy can easily be determined.

Figure 17 (a) and (b) shows the straight line tendency of linear rate constant (B/A) with 1/T. Using above equation activation energy has been calculated on both faces of 4H-SiC for wet oxidation as well as dry oxidation and are listed in table 3. Similarly, using parabolic rate constant the rate constants are plotted with 1/T (figure 18 (a) and (b)) and the activation energy on both terminating faces has been calculated and presented in table 3.

The linear rate constants B/A show the apparent activation energy of 2.81 eV (dry oxidation on Si-face), 2.274 eV (dry oxidation on C-face), 2.677 eV (wet oxidation on Si-face) and 2.131 eV (wet Oxidation C-face). Similarly parabolic rate constant B show the apparent activation energy of 2.86 eV (dry oxidation on Si-face), 2.0261 eV (dry oxidation on C-face), 2.505 eV (wet oxidation on Si-face) and 1.539 eV (wet Oxidation C-face). It has been found that the activation energy of C-face in both oxidations ambient is always less than that of Si-face, which clearly indicates a face terminated mechanism. Hence different oxidation rates on both faces of 4H-SiC, may be attributed to different activation energies found at both faces.

Activation energy (E_a)	Si-face (Dry oxidation)	C-face (Dry oxidation)	Si-face (Wet oxidation)	C-face (Wet oxidation)
From linear rate constant (B/A)	2.81 eV	2.274 eV	2.677eV	2.131 eV
From parabolic rate constant (B)	2.86 eV	2.0261 eV	2.505 eV	1.539 eV

Table 3. Experimentally measured value of Activation Energy (E_a) in linear region and parabolic region

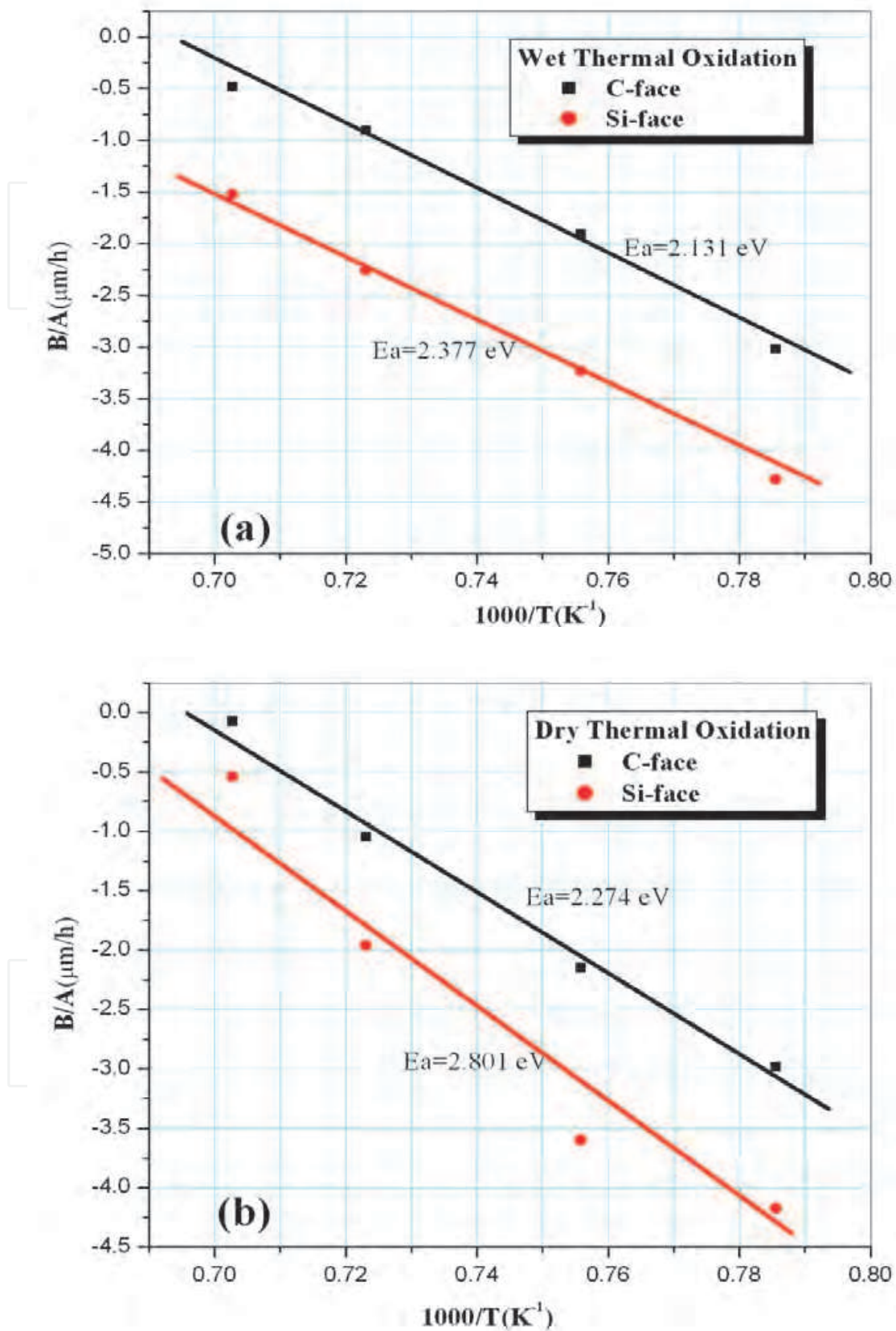Fig. 17. (a) Linear rate constant (B/A) as a function of 1/T for oxidation in wet ambient and (b) in dry ambient. Calculated activation energy is shown in their respective plots
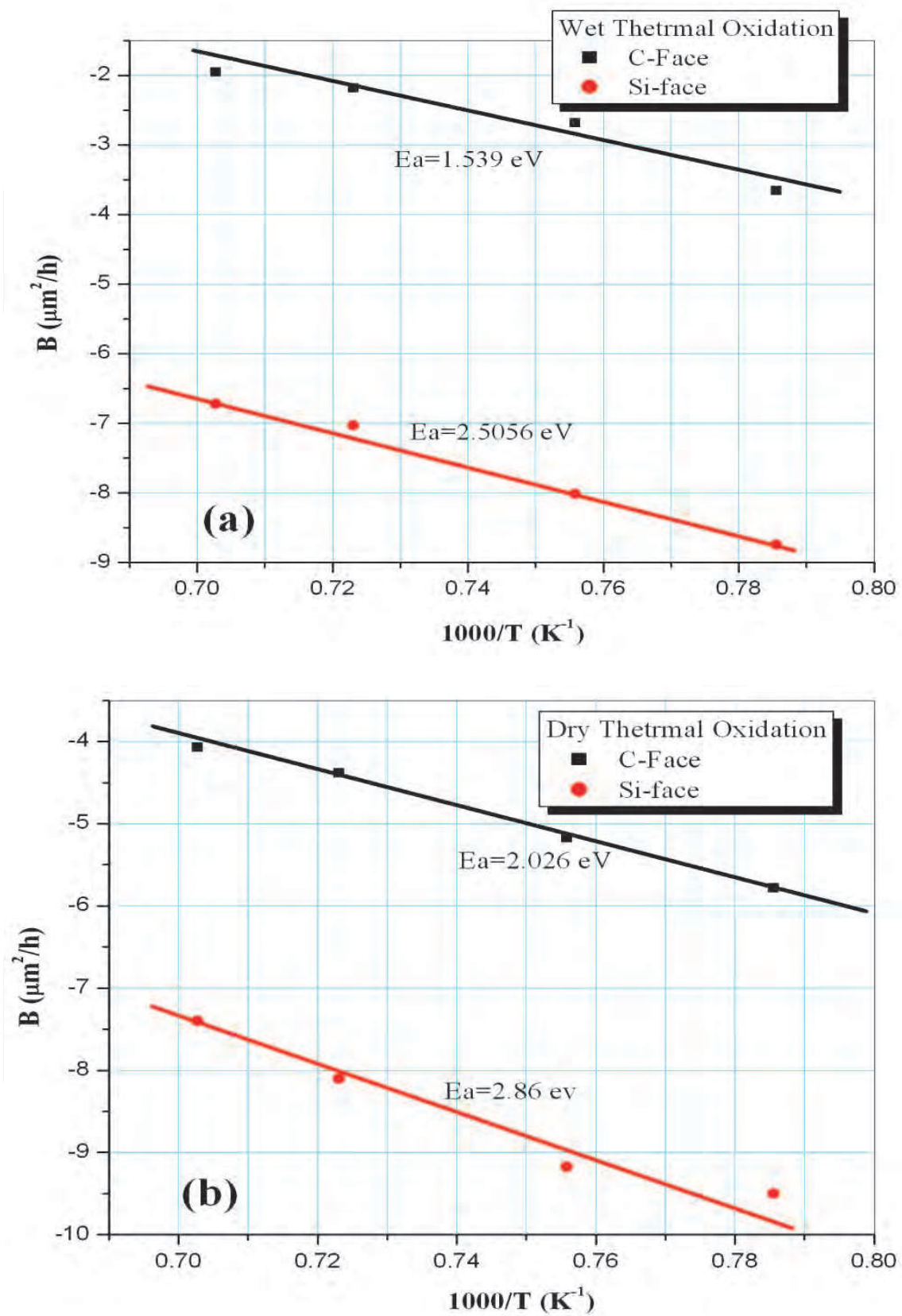
Fig. 18. (a) Parabolic rate constant (B) as a function of 1/T for oxidation in wet ambient and (b) in dry ambient. Calculated activation energy is shown in their respective plots

8. Conclusions

This chapter presents a systematically experimental study of the thermal oxide mechanism on 4H-SiC. On the basis of experimental results obtained, the following conclusions have been drawn.

- Thermal oxidation is a process that incorporates the interaction of molecular oxygen with oxidizing species, which are present on the substrate surface. The different mechanisms, through which oxygen is incorporated in the bulk and interface oxide regions during thermal oxidation of 4H-SiC, is namely the reaction with the SiC substrate and consumption of carbon clusters at both terminating faces.
- A face terminated oxidation behavior has been observed which indicates that the oxidation growth rate on C-face is faster than that of Si-face.
- In the thermal oxidation process of 4H-SiC, Si-face remains silicon rich face and C-face remains carbon rich face. This known observation indicates towards discrete nature of oxidation mechanism.
- The growth rate multiplication factor (GRMF) has been calculated for both oxidizing ambient (dry and wet). It has been concluded that in case of dry oxidation GRMF is found in the range of 4-6, means in case of dry oxidation C-face oxidize 4 to 6 times faster than that of Si-face. Similarly, for wet oxidation this GRMF is found in the range of 8-12, means in case of wet oxidation C-face oxidize 8 to 12 times faster than that of Si-face.
- It has been observed that the nature of growth rate is parabolic for all cases and initial average growth rate for wet oxidation is always faster than that of dry oxidation.
- It has been observed that the absolute value of rate constant (A) increases with decreasing oxidation temperature. At the same condition, the slope of the plots increases with increasing temperature means the value of rate constant B, increases with increasing temperature.
- The activation energy at both faces of 4H-SiC has been calculated using Arrhenius plots. It has been found that the activation energy of C-face for both oxidations ambient is always less than that of Si-face, which clearly indicates a face terminated mechanism.

9. References

[1] I. Vickridge, J. Ganem, Y. Hoshino and I. Trimaille, "Growth of SiO_2 on SiC by dry thermal oxidation: mechanisms", J. Phys. D: Appl. Phys. Vol. 40, pp. 6254-6263, 2007.

[2] Hiroshi Yano, Fumito Katafuchi, Tsunenobu Kimoto, and Hiroyuki Matsunami, "Effects of Wet Oxidation/Anneal on Interface Properties of Thermally Oxidized SiO_2 /SiC MOS System and MOSFET's", IEEE Trans. Electron Devices, Vol. 46, No. 3, pp. 504-510, 1999.

[3] K. Kamimura, D. Kobayashi, S. Okada, T. Mizuguchi, E. Ryu, R. Hayashibe, F. Nagaume and Y. Onuma, " Preparation and characterization of SiO_2/6H-SiC metal-insulator-semiconductor structure using TEOS as source materials", Appl. Surf. Sci., Vol. 184, Issue 1-4, pp. 346-349, 2001.

[4] P. T. Lai, J. P. Xu, H. P. Wu, C. L. Chen, "Interface properties and reliability of SiO$_2$ grown on 6H-SiC in dry O2 plus trichloroethylene", Microelectron. Reliab. Vol. 44, Issue 4, pp. 577-580, 2004.

[5] M. Meakawa, A. Kawasuso, Z. Q. Chen, M. Yoshikawa, R. Suzuki, T. Ohdaria, "Structural defect in SiO$_2$/SiC interface probed by a slow positron beam", Appl. Surf. Sci. Vol. 244, Issue 1-4, pp. 322-325, 2005.

[6] C. Zetterling, M. Ostling, C. I. Harris, P. C. Wood, S. S. Wong, "UV-ozone precleaning and forming gas annealing applied to wet thermal oxidation of p-type silicon carbide", Mater. Sci. Semicond. Process., Vol. 2, Issue 1, pp. 23-27, 1998.

[7] Eckhard Pippel and Jörg Woltersdorf, Halldor O. Oafsson and Einar O. Sveinbjornsson, "Interfaces between 4H-SiC and SiO$_2$: Microstructure, nanochemistry, and near-interface traps", J. Appl. Phys., Vol. 97, p. 034302, 2005.

[8] Mark Schürmann, Stefan Dreiner, Ulf Berges, and Carsten Westphal, "Investigation of carbon contaminations in SiO$_2$ films on 4H-SiC (0001)", J. Appl. Phys., Vol. 100, p. 113510, 2006.

[9] X. D. Chen, S. Dhar, T. Isaacs-Smith, J. R. Williams, L. C. Feldman,, and P. M. Mooney, "Electron capture and emission properties of interface states in thermally oxidized and NO-annealed SiO$_2$ /4H-SiC", J. Appl. Phys., Vol. 103,p. 033701, 2008.

[10] V. R. Vathulya. D. N. Wang and M. H. White, "On the correlation between the carbon content and the electrical quality of thermally grown oxide on p-type 6H-Silicon Carbide", Appl. Phys. Lett., Vol. 73, pp. 2161-2163, 1998.

[11] I.C.Vickridge, J. J. Ganem, G. Battisig, and E. Szilagyi, "Oxygen isotropic tracing study of the dry thermal oxidation of 6H-SiC", Nucl. Instrum. Methods Phys. Res., Vol.161B, pp. 462- 466, 2000.

[12] Y. Song, S. Dhar, L.C. Feldman, G. Chung, and J.R. Williams, "Modified deal and grove model for the thermal oxidation of silicon carbide", J. Appl. Phys., Vol. 95, pp. 4953-4957, 2004.

[13] J. M. Knaup, P. Deak, T. Frauenheim, A. Gali, Z. Hajnal, and W.J. Choyke, "Theoretical study of the mechanism of dry oxidation of 4H-SiC", Physical Review B Vol.71, pp.235321-235328, 2005.

[14] M. Schuermann, S. Dreiner, U. Berges and C. Westphal, "Structure of the interface between ultra thin SiO$_2$ film and 4H-SiC (0001)", Physical Review B Vol. 74, pp. 035309-035313, 2006.

[15] P. Fiorenza and V. Raineri, "Reliability of thermally oxidized SiO$_2$/4H-SiC by conductive atomic force microscopy", J. Appl. Phys., Vol 88. pp. 212112-212115, 2006.

[16] B.E. Deal and A.S. Grove, "General relationship of the thermal oxidation of silicon", J. Appl. Phys.,Vol. 36, p. 3770, 1965.

[17] Eckhard Pippel and Woltersfordf, "Interface between 4H-SiC and SiO$_2$; microstructure, nanochemistry and interface traps", J. Appl. Phys., Vol.97, p. 034302, 2005.

[18] D. Schmeiber, D. R. Batchelor, R. P. Mikolo, O. Halfmann and A. L-Spez, "Oxide growth on SiC (0001) surfaces", Appl. Surf. Sci. Vol 184, Issue 1-4, pp. 340-345, 2001.

[19] M. T. Htun Aung, J. Szmidt and M. Bakowski, "The study of thermal oxidation on SiC surface", J Wide Bandgap Material, Vol. 9. No. 4, pp. 313-318, 2002.

[20] R. Kosugi, K. Fukuda and K Arai, "Thermal oxidation of (0001) 4H-SiC at high temperature in ozone-admixed oxygen gas ambient", Appl. Phys. Lett. Vol. 83, p. 884, 2003.

[21] E. H. Nicollian and J. R. Brews, MOS (Metal Oxide Semiconductor) Physics andTechnology, John Wiley and sons, New York, p. 673, 1981.
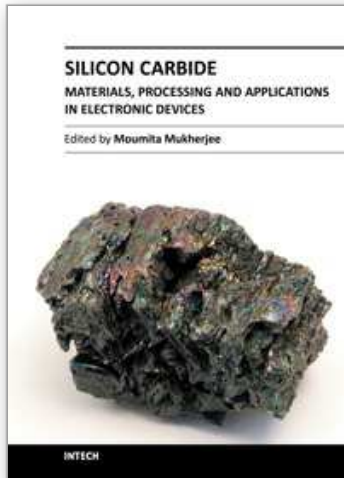
Silicon Carbide - Materials, Processing and Applications in Electronic Devices

Edited by Dr. Moumita Mukherjee

Silicon Carbide (SiC) and its polytypes, used primarily for grinding and high temperature ceramics, have been a part of human civilization for a long time. The inherent ability of SiC devices to operate with higher efficiency and lower environmental footprint than silicon-based devices at high temperatures and under high voltages pushes SiC on the verge of becoming the material of choice for high power electronics and optoelectronics. What is more important, SiC is emerging to become a template for graphene fabrication, and a material for the next generation of sub-32nm semiconductor devices. It is thus increasingly clear that SiC electronic systems will dominate the new energy and transport technologies of the 21st century. In 21 chapters of the book, special emphasis has been placed on the â€œmaterialsâ€ aspects and developments thereof. To that end, about 70% of the book addresses the theory, crystal growth, defects, surface and interface properties, characterization, and processing issues pertaining to SiC. The remaining 30% of the book covers the electronic device aspects of this material. Overall, this book will be valuable as a reference for SiC researchers for a few years to come. This book prestigiously covers our current understanding of SiC as a semiconductor material in electronics. The primary target for the book includes students, researchers, material and chemical engineers, semiconductor manufacturers and professionals who are interested in silicon carbide and its continuing progression.

INTECH
open science | open minds

Fax: +385 (51) 686 166   Fax: +86-21-62489821
www.intechopen.com